Fast 2D crack profile reconstruction by image processing for Eddy-Current Testing

G. Betta[1], L. Ferrigno[1], M. Laracca[1], H.G. Ramos[2], M. Ricci[3], A. L. Ribeiro[2], G. Silipigni[3]

[1] Dept. of Electric and Information Engineering - University of Cassino and Southern Lazio, Cassino, Italy
[2] Instituto de Telecomunicações - Instituto Superior Técnico, Lisboa, Portugal
[3] Dept. of Engineering, Polo Scientifico Didattico di Terni - University of Perugia, Terni, Italy
Email: m.laracca@unicas.it

***Abstract*— Fast reconstruction of defects geometry is one of the main goal of Eddy Current Non-destructive testing. The information about the type of defects, their shapes, orientations and geometrical characteristics is of great importance in evaluating the impact of defects on structures' integrity and operation safety. From one point of view, the knowledge of the defect shape could give important information about the manufacturing, the use or the cause that have stressed the specimen and generated the defect, and from the other point of view the reconstruction of geometrical parameters of defect could be made easier if the shape of the defect is known. Although many inverse procedures have been developed for Eddy Current Testing, usually high-computational time and resources are requested, hampering the application of 3D reconstruction methods in on-line or in-situ inspections. In this paper a fast 2D defect profile reconstruction technique is presented based on image processing. The main idea of the proposed method is that images obtained from the maps of magnetic field on specimen with flaws, express a trend attributable to a class of known functions. In particular, the shape of the obtained image depends on both the type of defect that the type of measurement probe adopted. Then using a suitable reference image related to the response of the probe as a digital filter to process the acquired image through deconvolution or correlation operations, the shape of the flaw that has generated the image can be retrieved.**

Keywords—Eddy Current Testing, Image Processing, Defect reconstruction

I. INTRODUCTION

Eddy Current Testing (ECT) is one of the most used Non-Destructive Testing (NDT) technique to inspect materials in aerospace applications. In particular, ECT is commonly utilized to inspect metallic non-ferromagnetic parts made of Aluminum, Titanium, Al-Li alloys or some austenitic alloys such as Inconel in order to detect cracks, corrosion, voids or residual stress.

Main tasks of a NDT-ECT inspection are the generation of suitable currents to be induced in the specimen, the measurement of suitable reaction fields and the collection and processing of measurement information over the specimen surface. Many excitation and measurement strategies have been implemented to optimize the sensitivity of the technique and proper probes and advanced signal processing techniques as well as information extraction procedures have been applied and reported in literature [1-6]. Although the various methods proposed can be significantly different, i.e. pulsed ECT Vs multi-frequency ECT, the final goal actually consists in providing images of the inspected samples and in reconstructing the 3D profile of defects when present. This profile can be in "gray-scale" when the 3D electrical conductivity distribution is reconstructed or in "B&W" (also called "ON/OFF") when every spatial point can be "sound" or "defect".

This shape profile assessment is very important for two reasons. From one point of view, the knowledge of the defect shape can give important information about the manufacturing or stress process that has generated the defect. On the other hand, the reconstruction of geometrical parameters of defect, can be made easier if the shape of the defect is known.

Actually, starting from measurements collected on proper grids of positions, the 3D ECT images are obtained by applying "inverse procedures" that can adopt deterministic or probabilistic methods. In the former case, the inverse procedure reckons on the exploitation of forward model solution, and, in general, iterative procedures are requested to produce 3D conductivity maps [7]. In the latter case, the 3D map is obtained by comparing the experimental measurements with database of previous experimental/ synthetic data [8], [9].

Deterministic inversion usually implies several computation of the forward model thus leading to relevant computational time/resources. This hampers the implementation of such inverse procedure in on-line inspection or in in-situ analysis, limiting therefore the application of ECT with respect to other NDT techniques. To face this issue, fast deterministic procedures have been recently proposed [10]. On the other hand, probabilistic inverse procedures usually rely on the individuation of proper features of the data to be used for forming the 3D conductivity maps. In this case computational time for performing the "inversion" can be compatible with on-line inspections but a huge work is in advance requested to create databases, to train the learning algorithms, to individuate features, etc.

Starting from the above mentioned considerations, a different approach for extracting the 2D defect profile of conductivity is proposed in this work. In particular, a fast method based on the image processing of the obtained ECT map is investigated for the reconstruction of the 2D x-y shape of defects.

M.R. and G.S. acknowledge financial support from Fondazione CARIT ("Electromagnetic techniques for Non-Destructive Evaluation of metallic structures ")

978-1-4799-7569-3/15/$31.00 ©2015 IEEE

The main idea of the proposed method is that images obtained from the maps of magnetic field on specimen with flaws, express a trend attributable to a class of known functions. In particular, the shape of the obtained image depends on both the type of defect that the type of measurement probe adopted. Then using a suitable reference image related to the response of the probe as a digital filter to process the acquired image through a deconvolution operation, the shape of the flaw that has generated the image can be retrieved. In the following, the theory which is the basis of the proposed method is explained in detail together with some preliminary experiments.

II. Fast defect profile reconstruction: state of the art

It is well known that information about defect's depth and height can be inferred by analyzing the frequency content of EC signals; to this regard various methods have been proposed that use multi-frequency or frequency-modulated excitations [2, 9, 11]. Moreover, recently, a fast method to reconstruct depth profiles of cracks has been developed by starting from time-domain Pulsed Eddy Current (PEC) data [12]. By contextually exploiting time and frequency information it is expected that a better accuracy in the defect depth profile reconstruction is reached; for this reason some of the authors proposed recently to use frequency modulated signals and pulse compression techniques to retrieve time and frequency information while optimizing simultaneously the SNR of the measurements. On the other hand, reconstruction of the 2D x-y cracks' profiles cannot be retrieved by time and frequency analysis but instead needs the processing of multiple acquisitions performed on grids of measurement points. Starting from these measurements, EC images are obtained by visualizing various quantities or features derived both from time and frequency analysis and by using various sensors such as pick-up coils, magnetic field sensors -Hall or GMR probes- or magneto-optic imaging techniques [13]-[22]. In all these cases a major problem in reconstructing the crack shape is represented by the diffusive nature of eddy currents. Indeed the presence of a defect modifies the magnetic B field in a quite large neighbor of the defect so that even a point defect produces a magnetic pattern with a significant spatial extension, this pattern being determined by both the excitation coil and the sensor used to measure the B field. It is therefore not straightforward determining the crack shape from ECT images, even for surface or near-surface defects but instead several classification methods have been reported that rely on the analysis of the magnetic patterns [9], [11]. These methods, although effective, suffer often from limited generality being based on specific properties of the current measurement set-up. In this paper, starting from a review of the literature, some common characteristic features of EC images are highlighted and related to well-known analytic functions, the Hermite-Gaussian modes. These functions are then used to process EC images for reconstructing the 2D crack profile by means of two different techniques: (i) image deconvolution, (ii) image correlation.

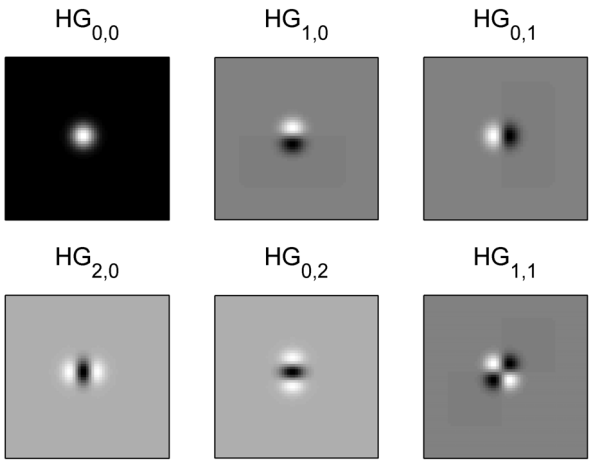

Figure 1: Hermite Gaussian (HG) patterns associated to various modes

III. Hermite-Gaussian Hypothesis

At the hearth of the present work lies the hypothesis that images of the B magnetic field variations produced by defects under ECT exhibit strong similarities with the 2D images of the Hermite-Gaussian modes (HG). Precisely we hypothesize that the Point-Spread-Function (PSF) that relate an "infinitesimal crack" (i.e. a crack with the minimum detectable dimensions) with its corresponding EC image is well described by a HG mode profile. The magnetic images of extended defects are then obtained by convoluting the defect

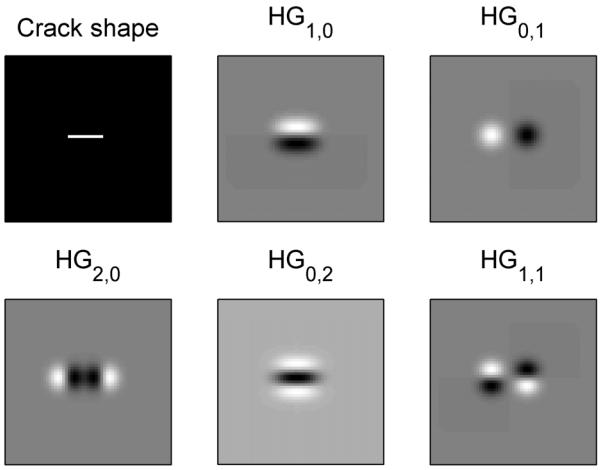

Figure 2: Magnetic patterns associated to a linear crack for various HG modes

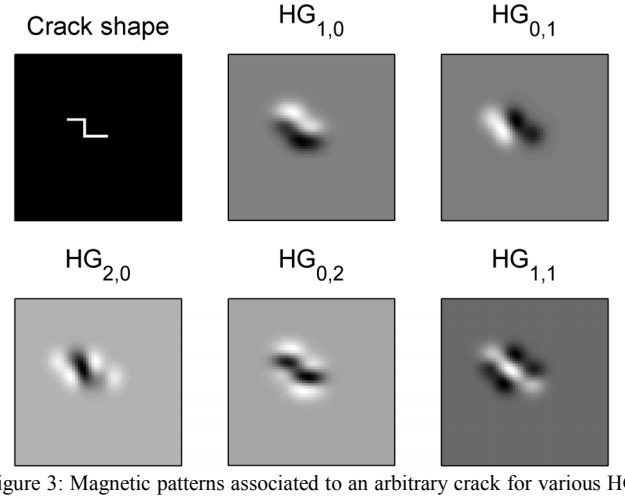

Figure 3: Magnetic patterns associated to an arbitrary crack for various HG modes

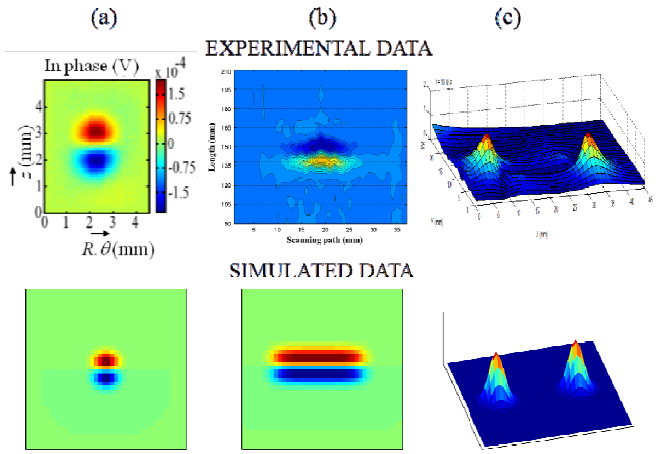

Figure 4. Comparison between experimental and theoretical images associated to $HG_{1,0}$ /$HG_{0,1}$ patterns: (a) small crack, see Fig.4 of [13], (b) long horizontal crack convolved with $HG_{1,0}$, see Fig.8 of [14]; (c) long horizontal crack convolved with $HG_{0,1}$, see Fig.5 of [15]

shape and the PSF. Moreover, it is well known that various measurement configurations lead to different EC images of the same defect, i.e. the PSF depends on the B component measured with sensors: we hypothesize that different measurement configurations correspond to different HG modes.

Hermite-Gaussian modes are extensively used in optics to describe the intensity profile of a laser beam when the wave equation is solved under the paraxial approximation. In particular, the 2D electric field distribution in the plane perpendicular to the direction of propagation is essentially given by the product of a 2D Gaussian function and a Hermite polynomial, apart from the phase term:

$$HG_{n,m}(x,y) = AH_n\left(\frac{\sqrt{2}}{w}x\right)H_m\left(\frac{\sqrt{2}}{w}y\right)e^{-(x^2+y^2)/w^2} \qquad (1)$$

where A is a constant, w is the spot size at the position z, H_n and H_m are the Hermite polynomials of order n and m

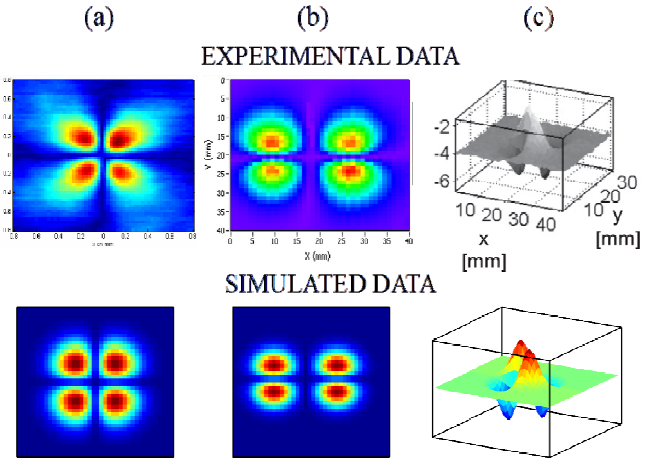

Figure 5. Comparison between experimental and theoretical images associated to $HG_{1,1}$ pattern: (a) very small crack, see Fig.9 of [16], (b) long horizontal crack convolved with $HG_{1,0}$, see Fig.8 of [17]; (c) long horizontal crack convolved with $HG_{0,1}$, see Fig.5 of [18]

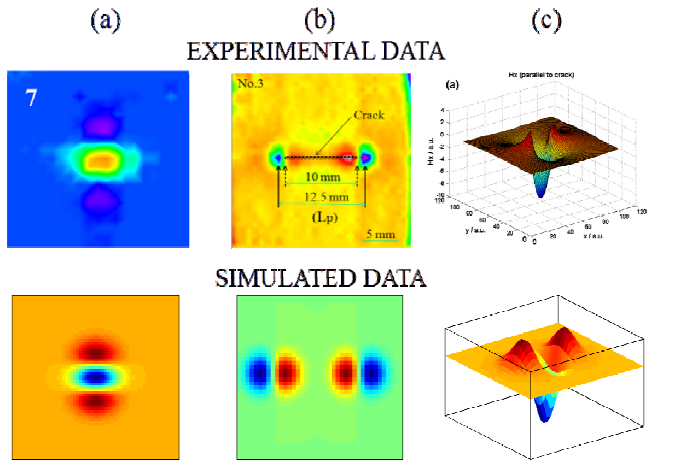

Figure 6. Comparison between experimental and theoretical images associated to $HG_{2,0}$ /$HG_{0,2}$ patterns: (a) small hole, see Fig.10 of [19], (b) long horizontal crack convolved with $HG_{2,0}$, see Fig.5 of [20]; (c) 3D image of crack convolved with $HG_{0,2}$, see Fig.6 of [21]

respectively [23]. For our purpose, it is sufficient to know that these are well-known polynomials which are the solution of a Sturm-Liouville eigenvalue problem [24]. For example, these functions turn up in the solution of the harmonic oscillator problem in quantum mechanics.

The first few Hermite polynomials are:

$$H_0(u) = 1, H_1(u) = 2u, H_2(u) = 4u^2 - 2, H_3(u) = 8u^3 - 12u \quad (2)$$

and in Figure 1 are reported the 2D patterns associated to HG modes of the lower orders ($HG_{0,0}$ coincide with a 2D Gaussian).

As said, if the defect covers several pixels of the obtained magnetic image, the basic assumption implies that the corresponding magnetic image is given by the 2D convolution between the crack shape and the PSF, as illustrated in Figures 2 and 3. Note that in this preliminary analysis, this assumption is valid for both surface and subsurface cracks, the only difference, as it will be better explained after, is that the PSF generally changes with the crack depth since for inner cracks low excitation frequencies must be used entailing a further spreading of the PSFs.

To corroborate the HG hypothesis, some examples of ECT images found in literature and corresponding to different modes are reported.

The images refer to cracks or small defects in sample with either planar or cylindrical geometry. In particular, Figure 4 reports some examples related to the Hermit-Gaussian modes $HG_{1,0}$ /$HG_{0,1}$, Figure 5 reports some examples related to the mode $HG_{1,1}$ and finally Figure 6 some example related to$HG_{2,0}$/$HG_{0,2}$. It is also worth to stress that different HG modes are related by partial derivative:

$$\frac{\partial HG_{n,m}(x,y)}{\partial x} = HG_{n+1,m}(x,y); \frac{\partial HG_{n,m}(x,y)}{\partial x} = HG_{n,m+1}(x,y); \qquad (3)$$

This properties is also exhibited by experimental data, further strengthen the Hermite-Gaussian Hypotesis, see for instance [19, 20, 25].

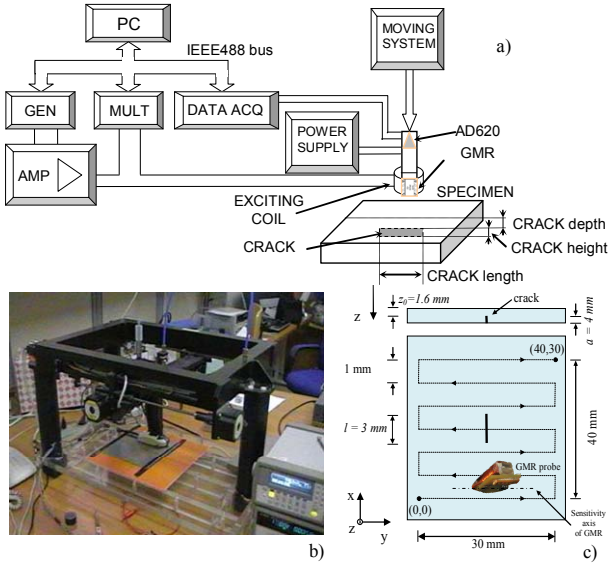

Figure 7. The developed measurement station (a), photo that highlights the precision moving system (b), sketch of the considered probe and specimen (c).

IV. First Experimental Results

Preliminary experimental results are shown in the following. They concern with tests executed on the measurement station of Figure 7. Key issue of the proposed test are the use of a measurement probe with exciting coil parallel to the plane of the specimen, and a GMR sensor always parallel respect to the plane of the specimen but orthogonal to the exciting coil. The considered specimen has a thin crack having the geometrical dimension reported in Figure 7c). A precision scanning system (Figure 7b) is able to move the probe on the specimen covering a map of 41x31 mm with a scanning resolution of 1 mm. The excitation is sinusoidal with a frequency equal to 2150 Hz.

Figure 8 shows the behavior of the magnetic field map as for the amplitude (a and b) and phase (c and d). The execution of a filtering and detrending stage allows the improvement of the obtained maps. The output of this stage is reported in Figure 9 a) and b) as for the amplitude and phase respectively.

Then the deconvolution stage is performed. In particular, Figure 10a) shows the deconvolution processing on the magnetic field amplitude map of figure 9a). The reference image is the Hermite-Gaussian function HG (1,1) highlighted in the square box of Figure 10a). Figure 10 b) and c) shows the results in terms of binarized images for the amplitude and phase magnetic field maps respectively.

It is possible to see that both the Figure 10b) and Figure 10c)

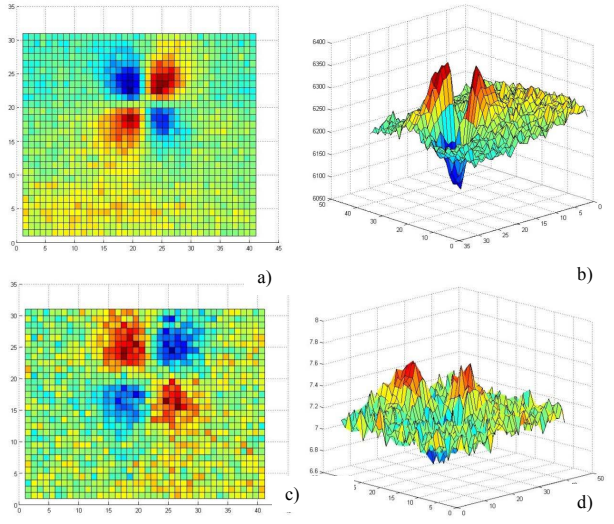

Figure 8. behavior of the magnetic field map as for the amplitude (a and b) and phase (c and d) for the considered specimen of Figure 7c). A frequency of 2150 Hz is considered.

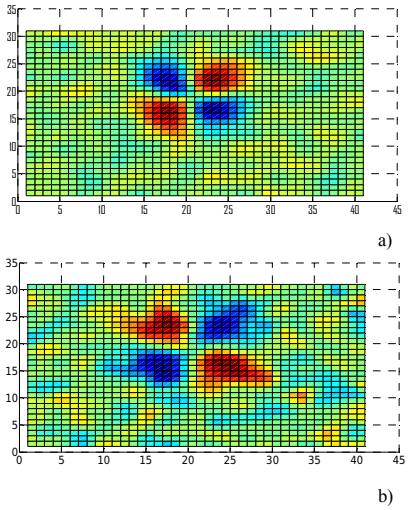

Figure 9. The output of the filtering and detrending stage for the amplitude (a) and phase (b) for the considered specimen of Figure 7c). A frequency of 2150 Hz is considered.

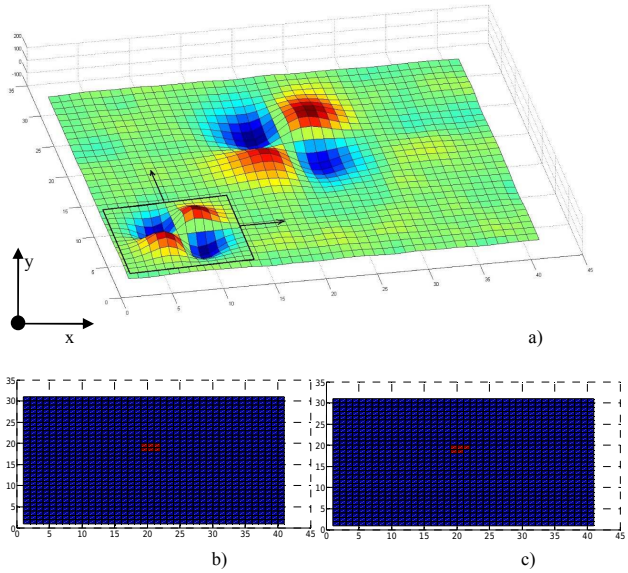

Figure 10. (a) deconvolution processing on the magnetic field amplitude map of figure 9a). The results in terms of binarized images for the amplitude (b) and phase(c) magnetic field maps.

correctly highlight the presence of a defect along the x-axis. As for the width of the detected defect it is strongly influenced by the scanning resolution (1 mm) and from the dimension of the exciting coil (1 cm). For this reason the defect appear wider than it is.

ACKNOWLEDGMENT

The authors thanks Fondazione CARIT for financial support, Pietro Burrascano for scientific discussions, and R. C. Menezes for his valuable help in the experimental tests.

This work was developed under the Instituto de Telecomunicações project Eval Tubes and supported in part by the Portuguese Science and Technology Foundation (FCT) project UID/EEA/50008/2013.

REFERENCES

[1] Lebrun, B., Jayet, Y., & Baboux, J. C. (1997). Pulsed eddy current signal analysis: application to the experimental detection and characterization of deep flaws in highly conductive materials. NDT & e international, 30(3), 163-170.

[2] Chady, T., Enokizono, M., & Sikora, R. (1999). Crack detection and recognition using an eddy current differential probe. Magnetics, IEEE Transactions on, 35(3), 1849-1852.

[3] Sophian, A., Tian, G. Y., Taylor, D., & Rudlin, J. (2002). Design of a pulsed eddy current sensor for detection of defects in aircraft lap-joints. Sensors and Actuators A: Physical, 101(1), 92-98.

[4] Burrascano, P., Carpentieri, M., Pirani, A., & Ricci, M. (2006). Galois sequences in the non-destructive evaluation of metallic materials. Measurement Science and Technology, 17(11), 2973.

[5] G. Betta, L. Ferrigno, M. Laracca, "GMR-based ECT Instrument for Detection and Characterization of Crack on Planar Specimen: a Hand-held Solution", IEEE Trans. Instrum. Meas., Vol. 61, No. 2, pp. 505-512, 2012

[6] Betta, G., Ferrigno, L., Laracca, M., Burrascano, P., Ricci, M., & Silipigni, G. (2015). An experimental comparison of multi-frequency and chirp excitations for eddy current testing on thin defects. Measurement, 63, 207-220.

[7] Pirani, A., Ricci, M., Specogna, R., Tamburrino, A., & Trevisan, F. (2008). Multi-frequency identification of defects in conducting media. Inverse Problems,24(3), 035011.

[8] Glorieux, C., Moulder, J., Basart, J., & Thoen, J. (1999). The determination of electrical conductivity profiles using neural network inversion of multi-frequency eddy-current data. Journal of Physics D: Applied Physics, 32(5), 616.

[9] Bernieri, A., Ferrigno, L., Laracca, M., & Molinara, M. (2008). Crack shape reconstruction in eddy current testing using machine learning systems for regression. Instrumentation and Measurement, IEEE Transactions on, 57(9), 1958-1968. 37-44.

[10] Tamburrino, A., Calvano, F., Ventre, S., & Rubinacci, G. (2012). Non-iterative imaging method for experimental data inversion in eddy current tomography.NDT & E International, 47, 26-34.

[11] A. Bernieri, G. Betta, L. Ferrigno, M. Laracca, "Crack Depth Estimation by Using a Multi-Frequency ECT Method," IEEE Transactions on Instrumentation and Measurement, Vol. 62, Issue: 3, pp. 544-552, 2013

[12] Bai, L., Tian, G. Y., Simm, A., Tian, S., & Cheng, Y. (2013). Fast crack profile reconstruction using pulsed eddy current signals. NDT & E International, 54,

[13] Joubert, P. Y., Vourc'h, E., & Thomas, V. (2012). Experimental validation of an eddy current probe dedicated to the multi-frequency imaging of bore holes.Sensors and Actuators A: Physical, 185, 132-138.

[14] He, Y., Pan, M., Luo, F., & Tian, G. (2011). Pulsed eddy current imaging and frequency spectrum analysis for hidden defect nondestructive testing and evaluation. Ndt & E International, 44(4), 344-352.

[15] Ramos, H., Postolache, O., Alegria, F. C., & Lopes-Ribeiro, A. (2009, May). Using the skin effect to estimate cracks depths in metallic structures. Proceedings of the IEEE Instrumentation and Measurement Technology Conference (I 2 MTC 2009) (pp. 1361-1366).

[16] Vacher, F., Gilles-Pascaud, C., Decitre, J. M., Fermon, C., Pannetier, M., & Cattiaux, G. (2006). Non destructive testing with GMR magnetic sensor arrays.Proc. 9th ECNDT, Berlin.

[17] Postolache, O., Ribeiro, A. L., & Ramos, H. G. (2013). GMR array uniform eddy current probe for defect detection in conductive specimens.Measurement, 46(10), 4369-4378.

[18] Betta, G., Ferrigno, L., Laracca, M., Burrascano, P., Ricci, M., & Silipigni, G. (2015). An experimental comparison of multi-frequency and chirp excitations for eddy current testing on thin defects. Measurement, 63, 207-220.

[19] Le, M., Lee, J., Jun, J., & Kim, J. (2013). Estimation of sizes of cracks on pipes in nuclear power plants using dipole moment and finite element methods.NDT & E International, 58, 56-63.

[20] Jun, J., Park, Y., & Lee, J. (2010). Real time visualization of alternating magnetic fields using 2-dimensional integrated Hall sensor array. J. Electr. Eng. Elektrotech. Casopis, 61(7), 32-35.

[21] Ribeiro, A. L., Ramos, H. G., & Postolache, O. (2012). A simple forward direct problem solver for eddy current non-destructive inspection of aluminum plates using uniform field probes. Measurement, 45(2), 213-217.

[22] D. J. Pasadas, A. Lopes Ribeiro, T. J. Rocha, Helena Geirinhas Ramos, Open Crack Depth Evaluation Using Eddy Current Methods and GMR Detection, IEEE MetroAerospace Procedings, Benevento, Italy, 2014.

[23] Kogelnik, H., and Tingye Li. "Laser beams and resonators." Applied Optics 5, no. 10, 1550-1567 (1966)

[24] Siegman, A. E. (1973). Hermite-Gaussian functions of complex argument as optical-beam eigenfunctions. JOSA, 63(9), 1093-1094.

[25] Le, M., Jun, J., Kim, J., & Lee, J. (2013). Nondestructive testing of train wheels using differential-type integrated Hall sensor matrixes embedded in train rails. NDT & E International, 55, 28-35.